Journal of Electroceramics 2:2, 119–125, 1998

Protonic Conduction in Perovskite-type Oxide Ceramics Based on $LnScO_3$ (Ln = La, Nd, Sm or Gd) at High Temperature

HIROAKI FUJII & YOSHIMASA KATAYAMA
Anan Kasei Co., 4-14-34 Fukaekita-machi, Higashinada-ku, Kobe 658, Japan

TETSUO SHIMURA & HIROYASU IWAHARA
Center for Integrated Research in Science and Engineering, Nagoya University, Furo-cho, Chikusa-ku, Nagoya 464-01 Japan

Submitted September 23, 1997; Revised December 24, 1997; Accepted January 7, 1988

Abstract. Ionic transport properties of perovskite-type oxides based on $LnScO_3$, $Ln_{1-x}Ca_xScO_{3-\alpha}$ (Ln = La, Nd, Sm and Gd) and $LaSc_{1-x}Mg_xO_{3-\alpha}$ were studied using an electrochemical method at elevated temperatures.

Conductivity in these oxide systems increased by more than three orders of magnitude upon doping with divalent atoms such as Ca or Mg. However, when $x \geq 0.1$, conductivities are almost independent of x in $La_{1-x}Ca_xScO_{3-\alpha}$ and $LaSc_{1-x}Mg_xO_{3-\alpha}$. $Gd_{0.9}Ca_{0.1}ScO_{3-\alpha}$ showed lower conductivity than $Ln_{1-x}Ca_xScO_{3-\alpha}$ (Ln = La, Nd and Sm).

Protonic conduction in these oxides under hydrogen containing atmospheres was confirmed by emf measurements of hydrogen concentration cells and by electrochemical hydrogen pumping using these oxides as a diaphragm. In $LaSc_{1-x}Mg_xO_{3-\alpha}$ the transport number of protons under hydrogen containing atmosphere was unity, suggesting that electronic conduction never became dominant, even under strong reducing conditions. Under condition of high oxygen partial pressure, the transport number of ions was less than 0.1, suggesting that the majority conductive carriers under such conditions were holes.

Keywords: proton conduction, perovskite, scandium oxide, concentration cell, electrochemical pump

1. Introduction

High temperature proton conducting solids are materials which have a great potential for application in high temperature devices. For example, this kind of solid is promising as a solid electrolyte material for hydrogen fuel cells. Hydrogen gas separation based on the principle of an electrochemical hydrogen permeation (pump) is also possible using a proton conducting solid. Deuteron separation may be another interesting application of proton conducting solids. In addition, this kind of protonic conductor can be used as a solid electrolyte for a hydrogen sensor. A sensor for *in situ* measurement of residual hydrogen in molten metal has already been commercialized [1].

For the application of proton conducting solids to such devices, high conductivity, as well as a high protonic transport number, is desirable. High chemical stability is also necessary. The most popular proton conducting solid, $BaCeO_3$-based ceramic, is not desirable from these points of view. At present, the discovery of a new proton conducting solid which has high protonic transport number and high chemical stability is required.

Since the discovery of high temperature protonic conduction in doped alkali earth cerates with perovskite-type structure $ACeO_3$, (A = Sr and Ba) [2,3], much investigation of high temperature proton conducting solids has been performed by many researchers. At present, high temperature protonic conduction is known in various materials such as $AZrO_3$ (A = Ca, Sr and Ba) [4,5], $KTaO_3$ [6,7],

$Ba_3Ca_{1+x}Nb_{2-x}O_9$ [8–10], $Ln_2Zr_2O_7$ [11], Sr_2TiO_4 [12] and $Ba_2SnYO_{5.5}$ [13]. All of these are complex oxides and have the following features.

(i) They all have a basic element like Ca, Sr, Ba, K or Ln as a component.
(ii) They all have oxygen octahedra, BO_6, with two- or three-dimensional linkages in their structure.
(iii) They exhibit high temperature protonic conduction when oxide ion vacancies are introduced by partial substitution of cations.

In the perovskite-type oxide protonic conductor described above, B site cations are Ce, Zr, Ti, (Ca + Nb), Ta and (Sn + Y). Besides these, scandium, Sc, could be considered as a candidate because of its suitable ionic size and good stability against reducing atmospheres. Recently, Kreuer [14] reported about the relation between stability of perovskite-type protonic conductors and lattice, tolerance factor $(r_A + r_O)/\sqrt{2}(r_B + r_O)$, where r_A, r_B and r_O are ionic radii of A-site ion, B-site ion and oxide ion, respectively. According to this relation, as the tolerance factor of lattice increases, the stability of perovskite-type oxide increases. The tolerance factor of $LaScO_3$ calculated using ionic radii estimated by Shannon [15] is 0.91, which is higher than that of $SrCeO_3$, 0.89. Therefore, the conduction in $LnScO_3$-based ceramics is worth investigating. In this paper, protonic conduction in a series of perovskite-type oxide ceramics based on $LnScO_3$ was studied. The samples examined here were $Ln_{1-x}Ca_xScO_{3-\alpha}$ (Ln = La, Nd, Sm and Gd) and $LaSc_{1-x}Mg_xO_{3-\alpha}$. In this experiment, Ca or Mg was used as a dopant for Ln or Sc, respectively.

2. Experimental

Ceramic samples of $Ln_{1-x}Ca_xScO_{3-\alpha}$ and $LaSc_{1-x}Mg_xO_{3-\alpha}$ were synthesized using a conventional solid state reaction method. Starting materials Ln_2O_3 (Ln = La, Nd, Sm and Gd), Sc_2O_3, $CaCO_3$ and MgO. Ln_2O_3 powders were baked at 1300°C before mixing to remove absorbed CO_2 and H_2O. Stoichiometric amounts of powders were mixed in an agate mortar with ethanol. The dried powder was then pressed into pellet shape with diameter of 15 mm and calcined at 1400°C for 10 h in air. Then pellets were cooled to room temperature in the furnace and reground using a ball mill with ethanol for 1 h. The reground powder was pressed into pellet shape by isostatic pressing at 200 MPa and sintering at 1650–1700°C for 10 h. Phase characterization of specimens was performed by X-ray diffraction analysis (XRD). Conduction properties of specimens were examined by electrochemical methods using the electrochemical cell described in [12]. The following measurements were carried out:

1. conductivity measurements using an a.c. two-probe method as a function of temperature or atmosphere at elevated temperatures (600–1000°C).
2. measurement of electromotive force (emf) of various concentration cells using the sample ceramics as an electrolyte.

$$Gas\ (I),\ Pt|Sample\ ceramic|Pt,\ Gas\ (II)$$

3. measurement of the hydrogen evolution rate from sample ceramics as a function of imposed current (electrochemical hydrogen pumping). In this experiment, direct current was passed through the concentration cell,

$$H_2,\ Pt|Sample\ ceramic|Pt,\ Ar$$

from anode (H_2) to cathode (Ar) and the hydrogen evolution rate was recorded as a function of current density, i. Hydrogen evolution rate at the cathode was determined by gas chromatography.

For all experiments, porous platinum was used for the electrode material. The atmosphere was controlled by changing the mixing ratio, (O_2, air or H_2)/Ar.

3. Results and Discussions

3.1. Prepared Samples

Figure 1 shows the XRD patterns of $LaScO_3$, $LaSc_{0.9}Mg_{0.1}O_{3-\alpha}$ and $Ln_{0.9}Ca_{0.1}ScO_{3-\alpha}$ (Ln = La, Nd, Sm and Gd). All diffraction peaks in each pattern were indexed assuming a $GdFeO_3$-type orthorhombic distorted perovskite-type unit cell. The existence of single phase was confirmed at $0 \leq x \leq 0.2$ both in $La_{1-x}Ca_xScO_{3-\alpha}$ and $LaSc_{1-x}Mg_xO_{3-\alpha}$ from the absence of impurity diffractions. As shown by splitting of diffraction peaks, the orthorhombic distortion in $Ln_{1-x}Ca_xScO_{3-\alpha}$ increased as the ionic radius of the A site (Ln site) ion decreased. Since no components in these oxides have d electrons, this increase of orthorhombic distortion originates only from the smaller ionic size of the A site ion. The relative densities of these oxides were between 90 and 95%.

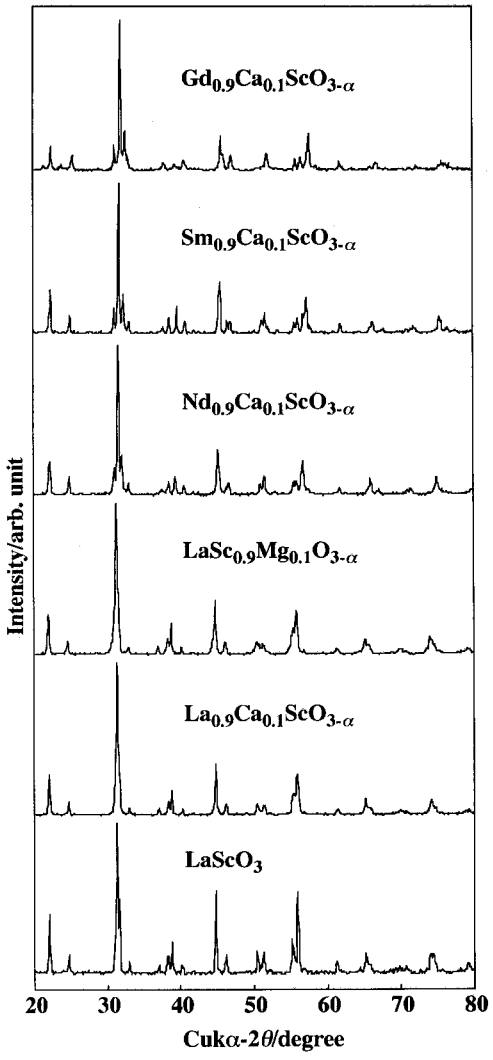

Fig. 1. XRD patterns of $LaScO_3$, $LaSc_{0.9}Mg_{0.1}O_{3-\alpha}$ and $Ln_{0.9}Ca_{0.1}ScO_{3-\alpha}$ (Ln = La, Nd, Sm and Gd).

3.2. *Conductivities*

Figures 2 and 3 show the Arrhenius plots of electrical conductivities of $La_{1-x}Ca_xScO_{3-\alpha}$ and $LaSc_{1-x}Mg_xO_{3-\alpha}$, respectively. As shown in Fig. 2, the electrical conductivity of non-doped $LaScO_3$ was very low so that measurement below 900°C was impossible. By substitution of Ca for La or Mg for Sc, conductivities increased by more than three orders of magnitude. At 1000°C, the conductivities in wet air were about one order of magnitude higher than that in hydrogen, as often observed in other high temperature protonic conductors [4,5,12]. This tendency is understood to originate from hole conduction. Figure 4 shows the conductivity of $La_{1-x}Ca_xScO_{3-\alpha}$ and $LaSc_{1-x}Mg_xO_{3-\alpha}$ at 900°C as a function of x. Except for $x = 0.05$, the conductivities of $La_{1-x}Ca_xScO_{3-\alpha}$ and $LaSc_{1-x}Mg_xO_{3-\alpha}$ were almost the same. For $La_{1-x}Ca_xScO_{3-\alpha}$, the dependence of conductivity on x was small in the region $0.05 \leq x \leq 0.2$. For $LaSc_{1-x}Mg_xO_{3-\alpha}$, the conductivity was apparently smaller when $x = 0.05$ as compared to $x \geq 0.1$.

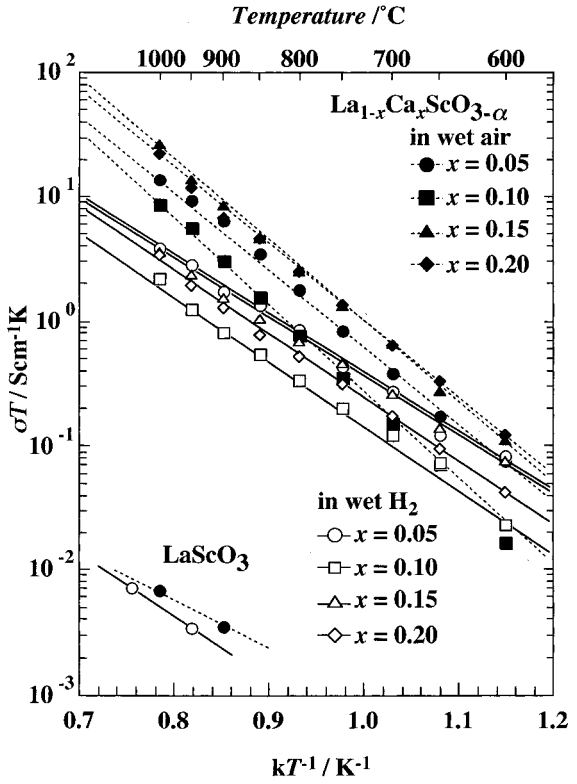

Fig. 2. Arrhenius plots of conductivities of $La_{1-x}Ca_xScO_{3-\alpha}$ ($0 \leq x \leq 0.20$) in wet air and in wet hydrogen.

Figure 5 shows the electrical conductivities of $Ln_{0.9}Ca_{0.1}ScO_{3-\alpha}$ (Ln = La, Nd, Sm and Gd) in wet air and in wet hydrogen in the form of an Arrhenius plot. Apparently, the conductivity of $Gd_{0.9}Ca_{0.1}ScO_{3-\alpha}$ was lower than that of $Ln_{0.9}Ca_{0.1}ScO_{3-\alpha}$ (Ln = La, Nd and Sm). Although the lattice distortion of $Gd_{0.9}Ca_{0.1}ScO_{3-\alpha}$ is larger than the distortions in $Ln_{0.9}Ca_{0.1}ScO_{3-\alpha}$ (Ln = La, Nd and Sm), this distortion is not the only cause of low conductivity. The conductivity of $Sm_{0.9}Ca_{0.1}ScO_{3-\alpha}$ was not lower than that of $Nd_{0.9}Ca_{0.1}ScO_{3-\alpha}$ and $La_{0.9}Ca_{0.1}ScO_{3-\alpha}$, in spite of the larger distortion

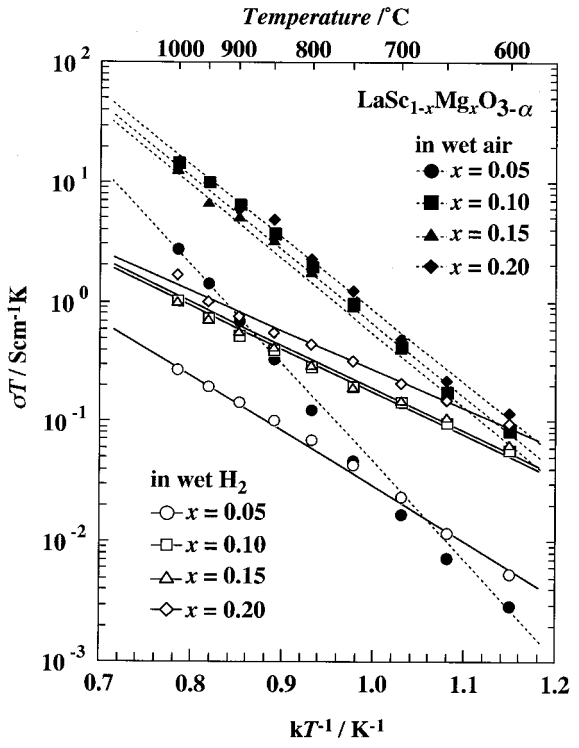

Fig. 3. Arrhenius plots of conductivities of $LaSc_{1-x}Mg_xO_{3-\alpha}$ $0.05 \leq x \leq 0.20$ in wet air and in wet hydrogen.

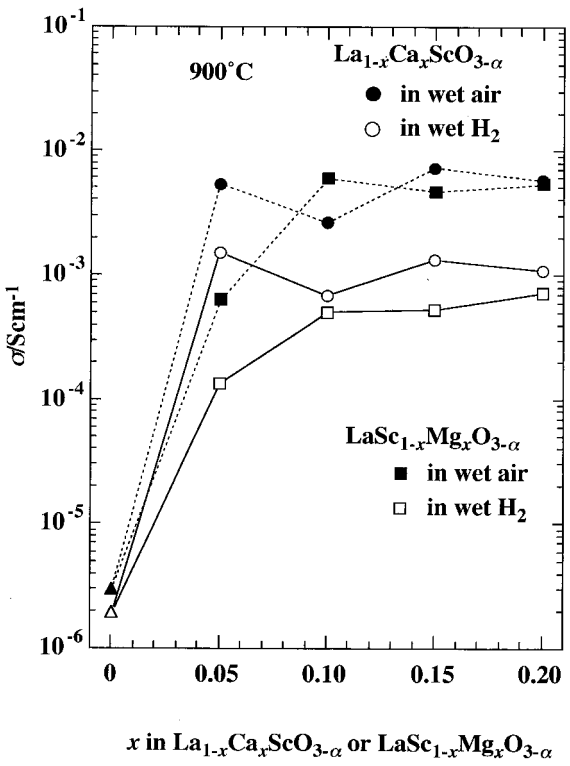

Fig. 4. Electrical conductivities of $La_{1-x}Ca_xScO_{3-\alpha}$ and $LaSc_{1-x}Mg_xO_{3-\alpha}$ at 900°C as a function of x.

of the lattice in $Sm_{0.9}Ca_{0.1}ScO_{3-\alpha}$ than in $La_{0.9}Ca_{0.1}ScO_{3-\alpha}$ and in $Nd_{0.9}Ca_{0.1}ScO_{3-\alpha}$. Rather, the low conductivity of $Gd_{0.9}Ca_{0.1}ScO_{3-\alpha}$ may be due to the low basicity of Gd compared to those of La ~ Sm. It is reported that the concentration of protons in the lattice decreases as the basicity of the oxide decreases [14].

To investigate the conduction behavior in these compounds, the dependence of conductivity on oxygen partial pressure was examined. Figure 6 shows the conductivities of $La_{0.9}Ca_{0.1}ScO_{3-\alpha}$ at 800, 900 and 1000°C as a function of oxygen partial pressure. Oxygen partial pressure was controlled by mixing ratio (wet O_2, wet air or wet hydrogen)/Ar. Under high oxygen partial pressure, the conductivities depend on oxygen partial pressure and the slopes, $\partial \log \sigma / \partial \log p_{O_2}$, at every temperature were close to 1/4, suggesting that, under high oxygen partial pressures, the concentration of oxygen vacancies was constant and the conduction was predominantly due to electron holes.

On the other hand, in the low oxygen partial pressure region, no increase in conductivity is observed. Although the scatter of experimental data was rather large, it was clear that any electronic conduction originating from the reduction of the component elements was not predominant even under a strongly reducing atmosphere at high temperature. The ionic conductivities of this oxide were 2.9×10^{-4}, 6.3×10^{-4} and 1.7×10^{-3} Scm^{-1} at 800, 900 and 1000°C, respectively. A similar tendency was also observed in the Mg substituted sample, $LaSc_{0.9}Mg_{0.1}O_{3-\alpha}$. This means that $LaScO_3$-based ceramics show *p*-type electronic/ionic mixed conduction at high oxygen pressure and pure ionic conduction at low oxygen partial pressure and elevated temperature.

The results shown in Fig. 6 suggest that in this oxide, the hole conductivity can be separately determined from the total conductivity (in wet air). Figure 7 shows the temperature dependence of hole conductivity between 700 and 1000°C in $La_{0.9}Ca_{0.1}ScO_{3-\alpha}$ with that of ionic and total conductivity. It is clear that in $La_{0.9}Ca_{0.1}ScO_{3-\alpha}$ the contribution of holes to the conductivity increases as

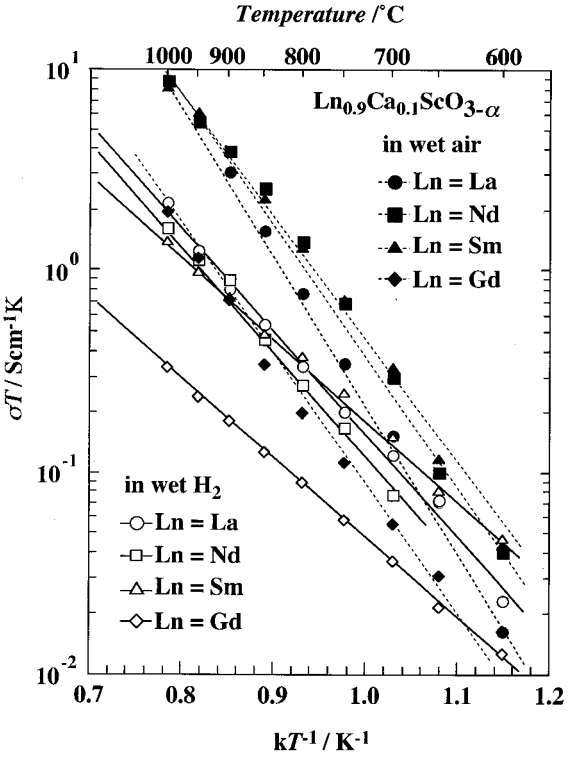

Fig. 5. Arrhenius plots of conductivities of $Ln_{0.9}Ca_{0.1}ScO_{3-\alpha}$ (Ln = La, Nd, Sm and Gd) in wet air and in wet hydrogen.

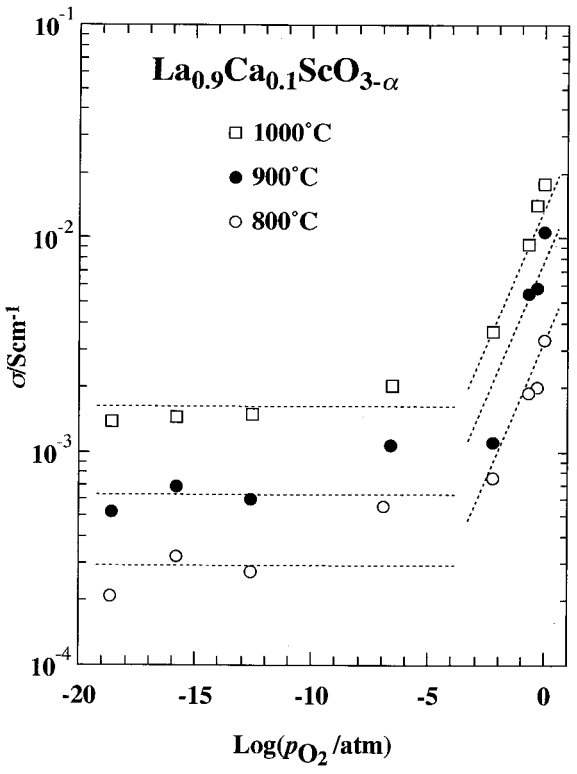

Fig. 6. Dependence of conductivity of $La_{0.9}Ca_{0.1}ScO_{3-\alpha}$ on oxygen partial pressure. The appearance of hole conduction under high oxygen partial pressure is clearly shown.

the temperature increases. The activation energy of hole conductivity between 700 and 900°C is 1.8 eV.

As a result, the enhancement of conductivity in $LaScO_3$-based ceramics by partial substitution for Ln or Sc site was confirmed. $Gd_{0.9}Ca_{0.1}ScO_{3-\alpha}$ showed lower conductivity than $Ln_{0.9}Ca_{0.1}ScO_{3-\alpha}$ (Ln = La, Nd and Sm), but this was impossible to explain solely by the large lattice distortion in $Gd_{0.9}Ca_{0.1}ScO_{3-\alpha}$.

3.3. Concentration Cells and Electrochemical Hydrogen Pump

To investigate the conduction mechanism in theses oxides, hydrogen and oxygen concentration cells using sample ceramics as diaphragms were constructed and their electromotive forces (emf) were measured. Figure 8 shows the emf of a hydrogen concentration cell at 700, 800 and 900°C using $LaSc_{0.9}Mg_{0.1}O_{3-\alpha}$ as a solid electrolyte.

$$H_2\ (1\ atm),\ Pt|LaSc_{0.9}Mg_{0.1}O_{3-\alpha}|Pt,\ H_2\ (pH_2)$$

Dashed lines express the theoretical emf at each temperature. As shown in the figure, the experimental values of emf were very close to the theoretical. Cells using other samples, for example $La_{0.9}Ca_{0.1}ScO_{3-\alpha}$, also exhibited emfs that were close to the theoretical values. Thus the ionic transport number in the sample under hydrogen containing atmosphere is almost unity, as expected from the dependence of conductivity on oxygen partial pressure. This suggests the possibility of a hydrogen sensor using this kind of Sc-containing perovskite-type oxides.

The observed emf of the oxygen concentration cell,

$$dry\ air,\ Pt|LaSc_{0.9}Mg_{0.1}O_{3-\alpha}|Pt,\ dry\ O_2\ (1\ atm)$$

is shown in Fig. 9 as a function of temperature. It is apparent that emf of this cell is far smaller than theoretical, indicating that, when hydrogen does not exist in the atmosphere (dry oxygen gas or dry air), hole conduction is predominant in these oxides. In wet air, on the other hand, contribution of ionic conductivity to the total one is relatively large, especially at low temperatures, as shown in Fig. 7. This suggests that

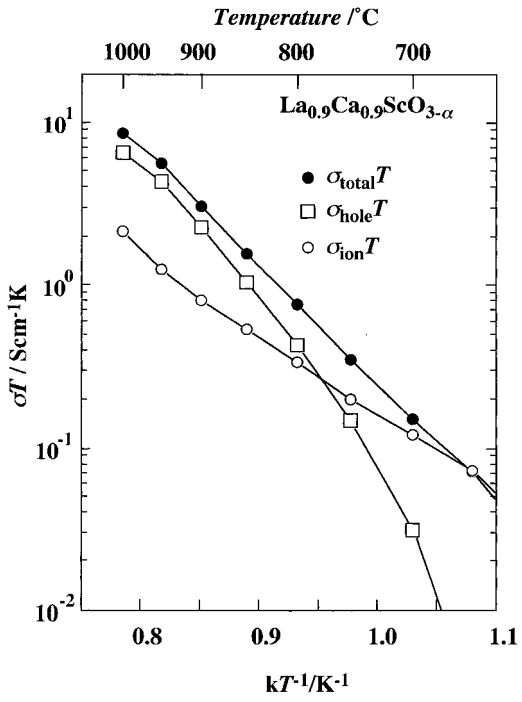

Fig. 7. Arrhenius plots of hole, ionic and total conductivity in $La_{0.9}Ca_{0.1}ScO_{3-\alpha}$.

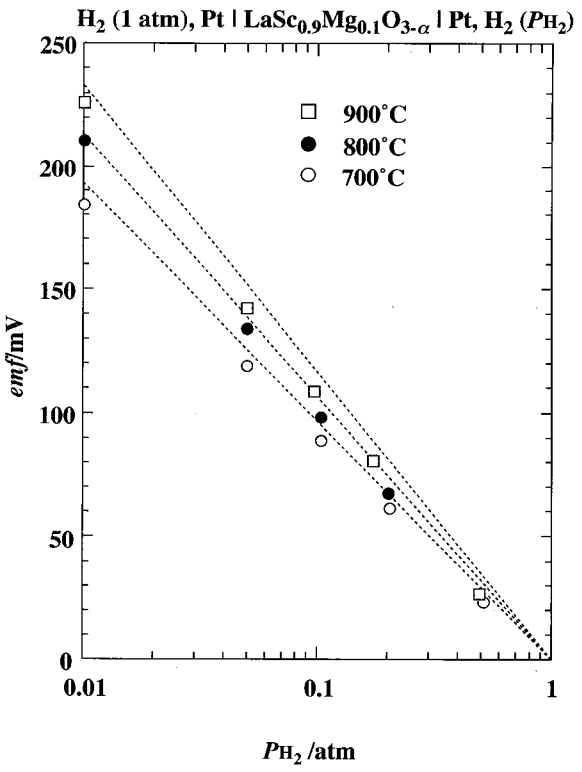

Fig. 8. Emf of a hydrogen concentration cell using $LaSc_{0.9}Mg_{0.1}O_{3-\alpha}$ as the solid electrolyte at 700, 800 and 900°C. Dashed lines indicate the theoretical emf at each temperatures.

the conductive ionic species in these oxides is protons.

To identify the mobile ion in these oxide directly, electrochemical hydrogen pumping was examined. Experiments were carried out at 900°C. The result is shown in Fig. 10. It is clear that, in the low current density region ($i \leq 20$ mAcm^{-2}), the hydrogen evolution rate increases monotonically with the current density. The slope (∂ hydrogen evolution rate/ ∂i) obeyed Faraday's law, suggesting that mobile ions under hydrogen containing atmosphere were protons.

On the other hand, in the high current density region the measured evolution rate showed saturation and then dropped. The origin of this saturation is not clear. One possibility is a limiting protonic current due to low hydrogen concentration at the interface between electrode material (Pt) and electrolyte. The drop might be due to the decomposition of the sample ceramic under a high imposed current.

4. Summary

Transport properties of $LaScO_3$ based perovskite-type oxides, $La_{1-x}Ca_xScO_{3-\alpha}$, $LaSc_{1-x}Mg_xO_{3-\alpha}$ and $Ln_{0.9}Ca_{0.1}ScO_{3-\alpha}$ (Ln = Nd, Sm and Gd) were investigated.

The existence of a single phase was confirmed for $La_{1-x}Ca_xScO_{3-\alpha}$ ($0 \leq x \leq 0.2$), $LaSc_{1-x}Mg_xO_{3-\alpha}$ ($0 \leq x \leq 0.2$) and $Ln_{0.9}Ca_{0.1}ScO_{3-\alpha}$ (Ln = Nd, Sm and Gd). The $GdFeO_3$-type lattice distortion increased with decreasing ionic radii of Ln ions.

An enhancement of conductivity by partial substitution of dopants for Ln or Sc site was observed. The dependence of conductivity on oxygen partial pressure showed that the dominant conductive carriers under hydrogen containing atmosphere were ions, but, under high oxygen partial pressure, the dominant carriers were electron holes. The emf measurement of gas concentration cells using $LaSc_{0.9}Mg_{0.1}O_{3-\alpha}$ as an electrolyte supported the above conduction behavior. The emf of hydrogen concentration cells agreed well with the theoretical values, suggesting pure ionic conduction under hydrogen containing atmosphere. Transport numbers of ions determined from the emf of oxygen concentration cells was very low.

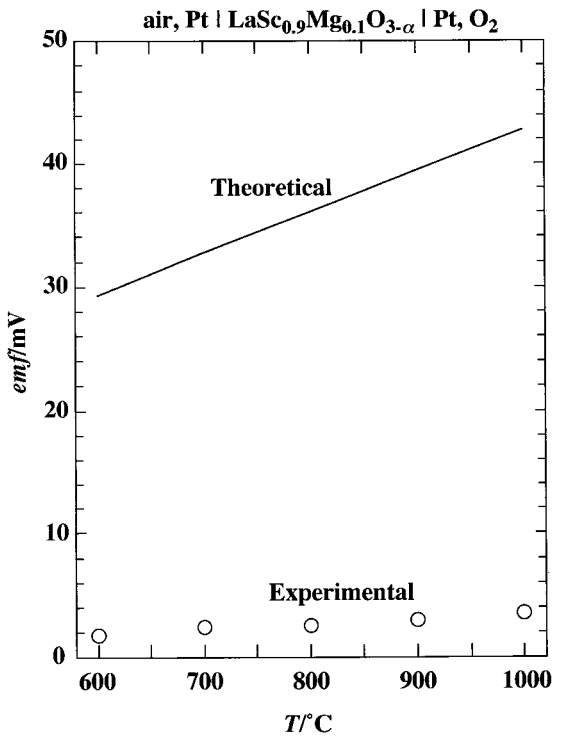

Fig. 9. Emf of an oxygen concentration cell using $LaSc_{0.9}Mg_{0.1}O_{3-\alpha}$ as the solid electrolyte; dry air ($PO_2 = 0.21$ atm), Pt|$LaSc_{0.9}Mg_{0.1}O_{3-\alpha}$|Pt, dry O_2($PO_2 = 1$ atm).

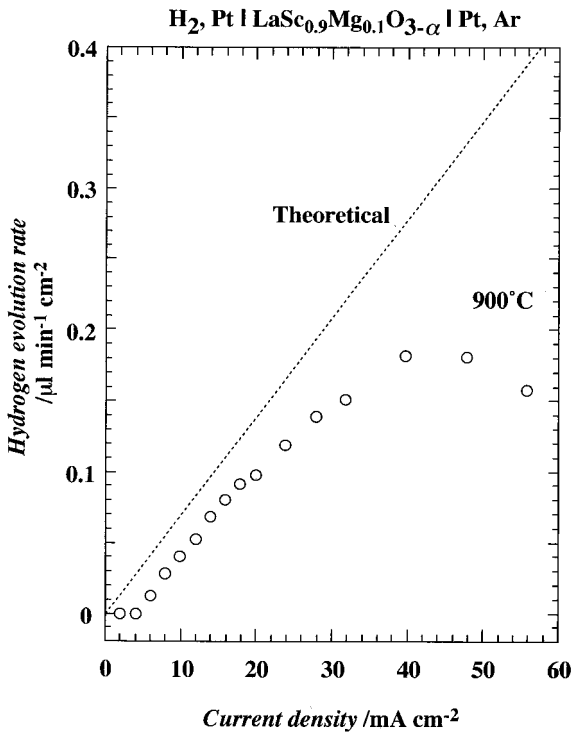

Fig. 10. The result of electrochemical hydrogen pumping using $LaSc_{0.9}Mg_{0.1}O_{3-\alpha}$. The straight line indicates the calculated evolution rate assuming that the transport number of protons is unity.

Proton conduction in $LaSc_{1-x}Mg_xO_{3-\alpha}$ was directly confirmed by electrochemical hydrogen pumping experiments. The dependence of hydrogen evolution rate on electrolytic current obeyed Faraday's law when the current density was less than 20 $mAcm^{-2}$, indicating that the charge carriers under this condition were protons.

Acknowledgment

A part of this study was supported by a grant-in-aid for Scientific Research in Priority Areas, '(No. 260), Dynamics of Fast Ions in Solids and Its Evolution for Solid State Ionics', from the Ministry of Education, Science, Sports and Culture, Japan.

References

1. T. Yajima, K. Koide, H. Takaki, N. Fukatsu, and H. Iwahara, *Solid State Ionics*, **79**,333 (1995).
2. H. Iwahara, T. Esaka, H. Uchida, and N. Maeda, *Solid State Ionics*, **3/4**, 359 (1981).
3. H. Iwahara, H. Uchida, K. Ono, and K. Ogaki, *J. Electrochem. Soc.*, **135**, 529 (1988).
4. T. Yajima, H. Kazeoka, T. Yogo, and H. Iwahara, *Solid State Ionics*, **47**, 271 (1991).
5. H. Iwahara, T. Yajima, T. Hibino, K. Ozaki, and H. Suzuki, *Solid State Ionics*, **61**, 65 (1993).
6. W.- K. Lee, A.S. Nowick, and L.A. Boatner, *Solid State Ionics*, **18/19**, 989 (1986).
7. T. Scherban, A.S. Nowick, L.A. Boatner, and M.M. Abraham, *Appl. Phys. A*, **55**, 324 (1992).
8. K.C. Liang and A.S. Nowick, *Solid State Ionics*, **61**, 77 (1993).
9. K.C. Liang, Y. Du, and A.S. Nowick, *Solid State Ionics*, **69**, 117 (1994).
10. A.S. Nowick and Y. Du, *Solid State Ionics*, **77**, 137 (1995).
11. T. Shimura, M. Komori, and H. Iwahara, *Solid State Ionics*, **86–88**, 685 (1996).
12. T. Shimura, K. Suzuki, and H. Iwahara, *Solid State Ionics*, in press.
13. P. Murugaraj, K.D. Kreuer, T. He, T. Schober, and J. Maier, *Solid State Ionics*, **98**, 1 (1997).
14. K.D. Kreuer, *Solid State Ionics*, **97**, 1 (1997).
15. R.D. Shanon, *Acta Crystallogr. B*, **92**, 972 (1970).